

A. Uchino  
Y. Takase  
K. Nomiyama  
R. Egashira  
S. Kudo

## Acquired lesions of the corpus callosum: MR imaging

Received: 6 May 2005  
Revised: 9 September 2005  
Accepted: 20 September 2005  
Published online: 12 November 2005  
© Springer-Verlag 2005

A. Uchino (✉) · Y. Takase ·  
K. Nomiyama · R. Egashira · S. Kudo  
Department of Radiology,  
Saga Medical School,  
5-1-1 Nabeshima,  
Saga 849-8501, Japan  
e-mail: [uchino@cc.saga-u.ac.jp](mailto:uchino@cc.saga-u.ac.jp)  
Tel.: +81-952-34-2309  
Fax: +81-952-34-2016

**Abstract** In this pictorial review, we illustrate acquired diseases or conditions of the corpus callosum that may be found by magnetic resonance (MR) imaging of the brain, including infarction, bleeding, diffuse axonal injury, multiple sclerosis, acute disseminated encephalomyelitis, Marchiafava-Bignami disease, glioblastoma, gliomatosis cerebri, lymphoma, metastasis, germinoma, infections, metabolic diseases, transient splenial lesion, dilated Virchow-Robin spaces, wallerian

degeneration after hemispheric damage and focal splenial gliosis. MR imaging is useful for the detection and differential diagnosis of corpus callosal lesions. Due to the anatomical shape and location of the corpus callosum, both coronal and sagittal fluid-attenuated inversion recovery images are most useful for visualizing lesions of this structure.

**Keywords** Corpus callosum · Acquired lesion · Magnetic resonance imaging

### Introduction

The corpus callosum is a large white matter tract connecting the two cerebral hemispheres. Thus, numerous connecting fibers pass through the corpus callosum. Recently developed diffusion tensor imaging is useful for the identification of these fiber tracts [1]. The fibers comprising the corpus callosum are more dense than those of the periventricular or deep white matter. The corpus callosum can be involved in many acquired diseases and conditions. Patients with a callosal lesion usually have severe clinical symptoms. Thus, the differential diagnosis of these lesions by means of magnetic resonance (MR) imaging is clinically important.

The purpose of this pictorial review is to describe the various types of acquired lesions that can appear in the corpus callosum on MR images. To our knowledge, there are few previous reports on this topic [2, 3]. We reviewed images obtained from many patients with acquired corpus callosal lesions diagnosed by MR imaging. These images included conventional spin-echo T1-weighted, spin-echo or fast spin-echo T2-weighted and fast fluid-attenuated inversion recovery (FLAIR) images obtained by various 1.5- or

1.0-T scanners. In some patients, proton-density (PD)-weighted, T2\*-weighted or diffusion-weighted images were also obtained. Axial images were usually obtained, and coronal or sagittal images were obtained occasionally.

### Vascular lesions

#### Infarction

The anterior half of the corpus callosum is supplied by the pericallosal artery, a branch of the anterior cerebral artery. According to a microsurgical anatomic study, the anterior communicating artery gives rise to either a subcallosal artery or a median callosal artery, each of which makes a substantial contribution to the blood supply of the corpus callosum [4]. The posterior half is supplied by the posterior pericallosal artery, a branch of the posterior cerebral artery. The vascular supply to the central zone of the genu and body of the corpus callosum, via short penetrating arterioles, is similar to that of the cerebral cortex, whereas the vascular supply to the centrum semiovale and basal ganglia is carried substantially by long endarteries [5]. Because of the rich blood supply, a

**Fig. 1** Corpus callosum infarct in a 57-year-old woman.

**a, b** Diffusion-weighted (TR/TE=4,000/101,  $b=1,000$ , 1.5 T) and fluid-attenuated inversion recovery (FLAIR) (TR/TI/TE=10,002/2,200/125) axial images obtained 9 days after onset show hyperintense lesions in the left side of the splenium of the corpus callosum and left occipital lobe, indicative of acute infarction of the left posterior cerebral artery territory

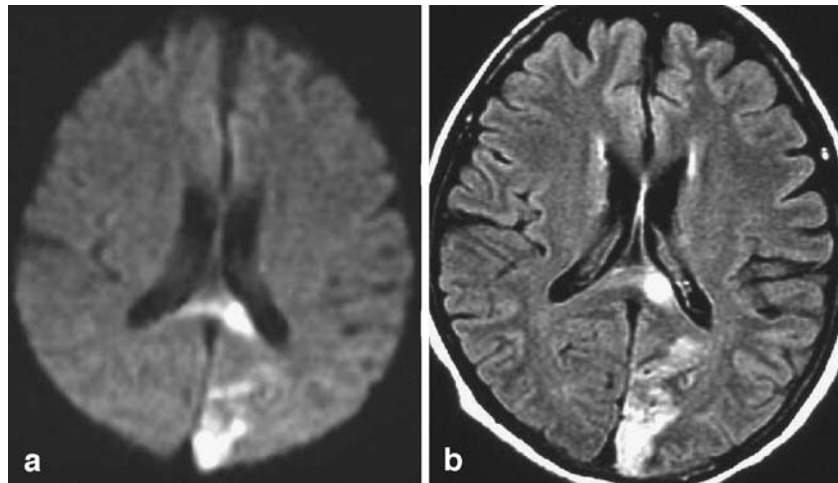
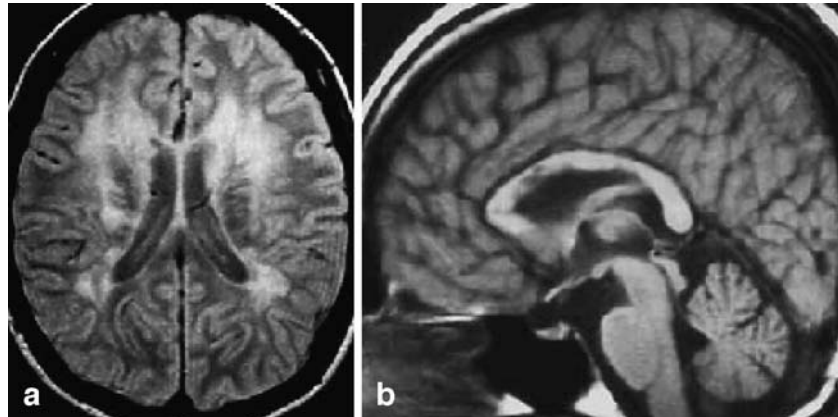


**Fig. 2** Cerebral autosomal dominant arteriopathy with subcortical infarcts and leukoencephalopathy in a 44-year-old woman. **a** Proton density-weighted axial image (TR/TE=2,500/20, 1.0 T) shows widespread lesions in the thalamus, basal ganglia and white matter. **b** T1-weighted midsagittal image (TR/TE=500/20) shows small lesions in the corpus callosum

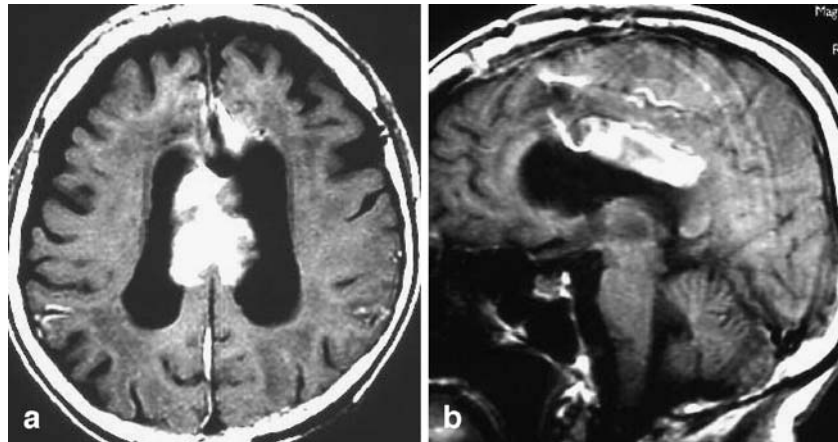


solitary infarct of the corpus callosum is not common, and it may be misdiagnosed as a brain tumor [6]. The most common location of callosal infarction is the splenium, followed by the body and genu [7]. Infarcts of the corpus callosum are usually associated with infarcts of the neighboring structures (Fig. 1). The corpus callosum is occasionally affected in patients with cerebral autosomal

dominant arteriopathy with subcortical infarcts and leukoencephalopathy (CADASIL) (Fig. 2). In patients with CADASIL, widespread lesions are observed including in the anterior temporal and superior frontal subcortical white matter [8]. The clinical history and distribution of the lesion are important in the correct diagnosis of corpus callosum infarcts.

**Fig. 3** Ruptured distal anterior cerebral artery (ACA) aneurysm in an 86-year-old woman.

**a, b** T1-weighted axial and midsagittal images (TR/TE=500/9, 1.5 T) obtained 1 month after onset show a large hematoma in the body of the corpus callosum. The ruptured distal ACA aneurysm has already been clipped surgically



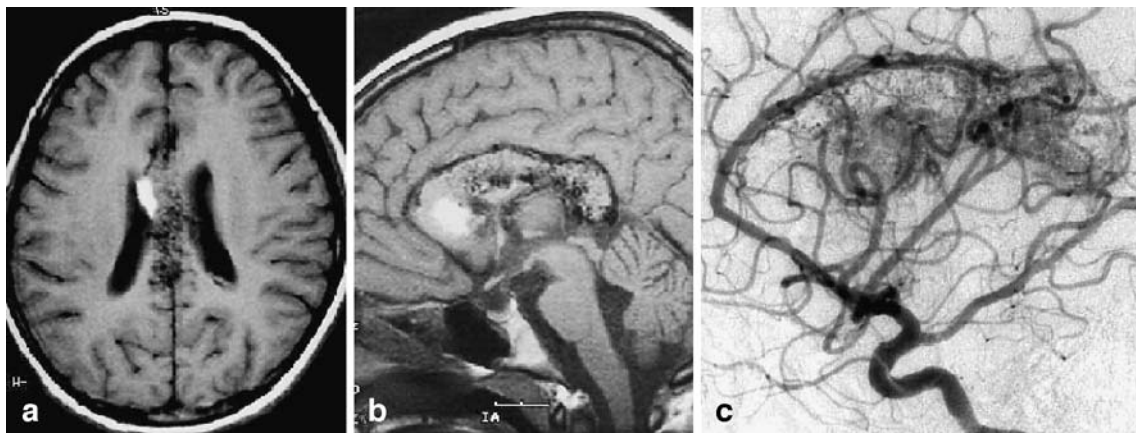


**Fig. 4** Ruptured arteriovenous malformation (AVM) of the corpus callosum in a 12-year-old girl. **a, b** T1-weighted axial and midsagittal images (TR/TE=450/9, 1.5 T) obtained 8 days after onset show a

hematoma in the genu of the corpus callosum. **c** Selective cerebral angiogram shows an extensive callosal AVM

#### Bleeding

Rupture of an aneurysm of the anterior communicating artery or distal anterior cerebral artery may cause hematoma in the corpus callosum (Fig. 3). Usually, the hematoma is associated with subarachnoid hemorrhage seen mainly in the interhemispheric cistern. A so-called callosal arteriovenous malformation may also cause hematoma in the corpus callosum (Fig. 4). Hypertensive cerebral hemorrhage is usually not seen in the corpus callosum.

#### Traumatic lesions

Lesions due to diffuse axonal injury are seen mainly in the corpus callosum, midbrain and corticomedullary junction of the cerebrum (Figs. 5, 6). Corpus callosal lesions are most commonly observed within the posterior body and splenium, and callosal injury in children does not necessarily indicate a poor prognosis [9]. FLAIR images are useful for the diagnosis of such callosal injury [10]. With the use of diffusion-weighted images, traumatic lesions can be classified as one of three types: vasogenic edema,

cytotoxic edema or central hemorrhagic lesion [11]. T2\*-weighted images are useful for the detection of associated microhemorrhage within the lesion.

#### Demyelinating lesions

##### Multiple sclerosis

The principal pathology of multiple sclerosis lesions is an inflammatory demyelinating process. The lesions are typically small, oval or round, and located in the deep white matter (Fig. 7). The corpus callosum is frequently affected, and lesions characteristically involve the inferior aspect of the callosum and radiate from the ventricular surface into the overlying callosum. These callosal-septal interface lesions are highly sensitive and specific for multiple sclerosis, and both sagittal and coronal PD-weighted images are useful for lesion detection [12, 13]. At our institution, FLAIR images are now obtained instead of PD-weighted images. Sagittal, thin-section, fast FLAIR images are useful for the detection of subcallosal striations, which are known to be early features of multiple sclerosis [14].

**Fig. 5** Diffuse axonal injury in a 79-year-old man. **a, b** FLAIR axial and midsagittal images (TR/TI/TE=10,000/2,200/125, 1.5 T) obtained 5 days after head injury show lesions in the posterior half of the corpus callosum. The midbrain, cingulate gyrus and both frontal lobes are also involved

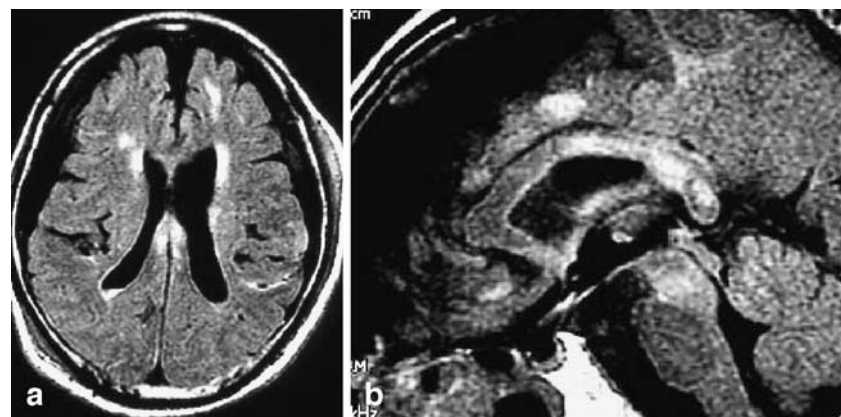


**Fig. 6** Injuries sustained by a physically abused 1-year-old boy. **a, b** A T2-weighted axial image (TR/TE=2,000/80, 1.5 T) and T1-weighted midsagittal image (TR/TE=400/20) show cavitary lesions in the body and splenium of the corpus callosum, indicative of head injury sequelae. The interval from the time of trauma to the time of image acquisition is unknown

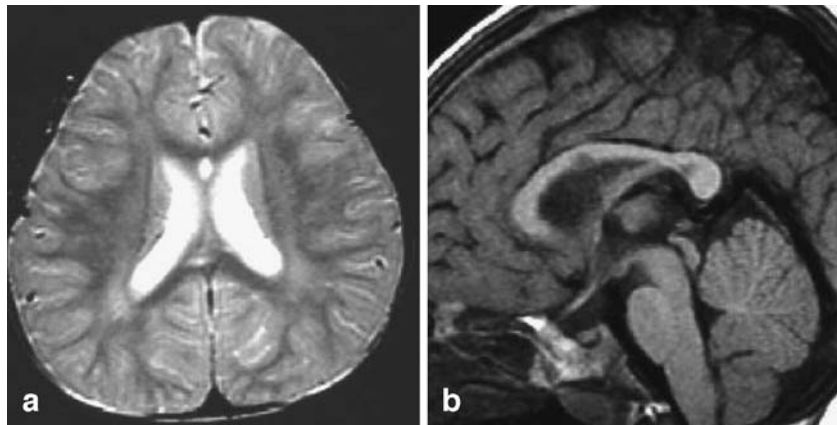
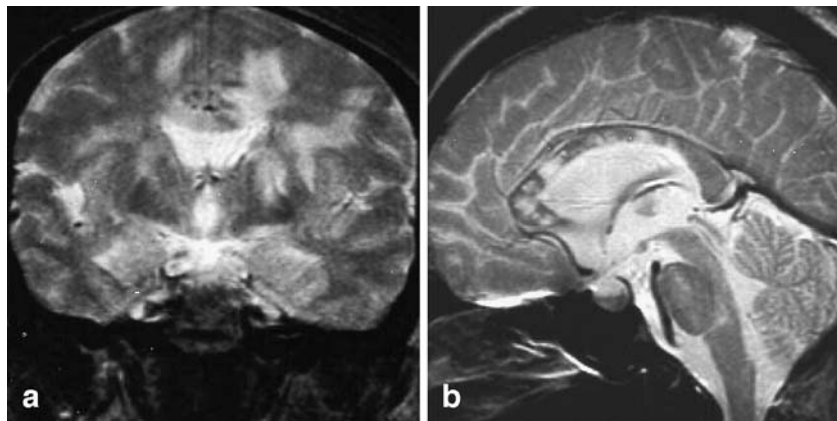


**Fig. 7** Images obtained 3 years after onset of multiple sclerosis in a 51-year-old woman. **a, b** T2-weighted coronal and midsagittal images (TR/TE=2,000/80, 1.5 T) show multiple oval and confluent lesions in the white matter and multiple small lesions in the corpus callosum

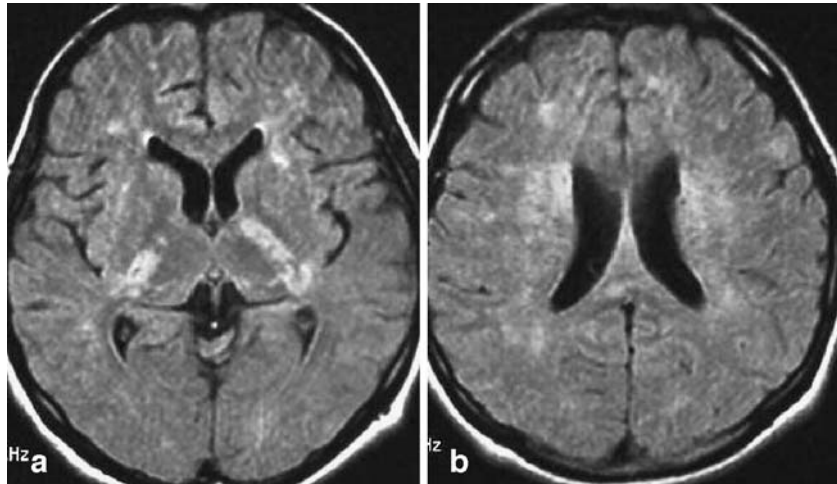


#### Acute disseminated encephalomyelitis

Acute disseminated encephalomyelitis is regarded as a postinfectious autoimmune disease. The clinical course is monophasic, and some patients recover completely [15]. MR imaging features are similar to those of multiple sclerosis

(Fig. 8). However, Brass et al. [16] reported that demyelinating lesions were more commonly located in the corpus callosum and the periventricular area in pediatric patients with multiple sclerosis than in patients with acute disseminated encephalomyelitis. Thus, the clinical history and radiological data are very important for a correct diagnosis.

**Fig. 8** Images obtained 3 months after onset of acute disseminated encephalomyelitis in a 20-year-old woman. **a, b** FLAIR axial images (TR/TE=10,002/2,200/133, 1.5 T) show multiple lesions in the white matter including the corpus callosum



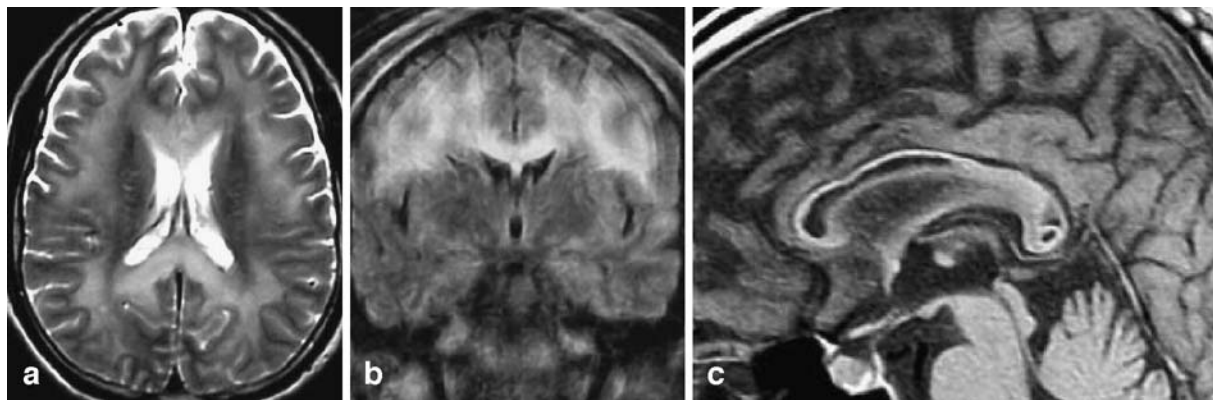


**Fig. 9** Marchiafava-Bignami disease in a 49-year-old man with chronic alcoholism. **a, b** T2-weighted axial (TR/TE=4,000/107, 1.0 T) and FLAIR coronal images (TR/TI/TE=8,000/2,200/120) obtained in the acute stage show diffuse white matter abnormality including the entire corpus callosum. **c** T1-weighted midsagittal

(TR/TE=500/10) image obtained 6 months after onset shows cavitary lesions in the corpus callosum. The peripheral layer of the corpus callosum is spared, resulting in the sandwich-like appearance

### Marchiafava-Bignami disease

Marchiafava-Bignami disease is a rare demyelinating disease of the corpus callosum most often seen in patients with chronic alcoholism. The disease is due mainly to a deficiency of the vitamin B complex, but the reason the corpus callosum is affected is not known. The corpus callosum degenerates and splits into three layers, a condition called “layered necrosis.” The middle layer of the corpus callosum is most severely involved, and the periphery is spared, resulting in a sandwich-like appearance. The demyelination may extend laterally into the neighboring white matter [17]. In the chronic stage, the affected corpus callosum becomes atrophic, and the middle layer becomes cavitary (Fig. 9).

### Neoplastic lesions

#### Glioblastoma

Glioblastoma is commonly found in the supratentorial white matter including the corpus callosum. This aggressive tumor spreads via direct extension along white matter tracts. The corpus callosum is frequently involved. When it extends bilaterally into the cerebral hemispheres, the tumor is called “butterfly glioblastoma.” The characteristic MR feature of glioblastoma is heterogeneous enhancement with central necrosis (Fig. 10).

#### Gliomatosis cerebri

Diffuse benign glioma, called gliomatosis cerebri, may affect the corpus callosum. Fibrillary astrocytoma is the

**Fig. 10** Glioblastoma in a 59-year-old man. **a** FLAIR axial image (TR/TI/TE=10,002/2,200/133, 1.5 T) shows a massive bilateral frontal lobes lesion, including the corpus callosum. **b** Post-contrast T1-weighted coronal image (TR/TE=616/12) shows focal enhancement with central necrosis, indicative of “butterfly glioblastoma”

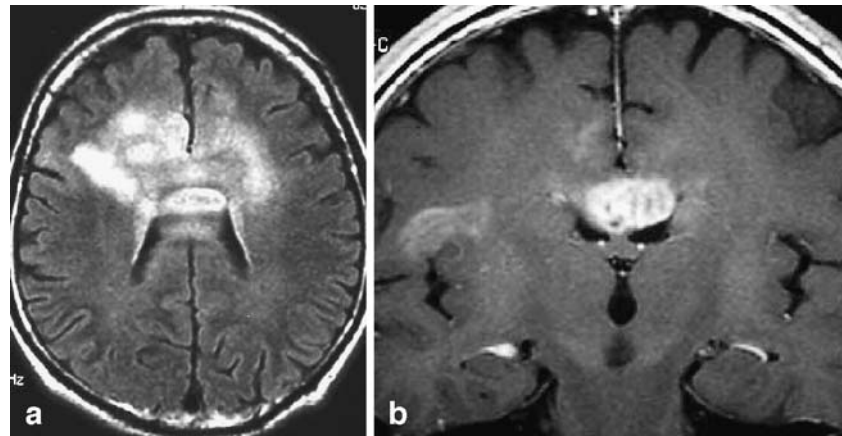
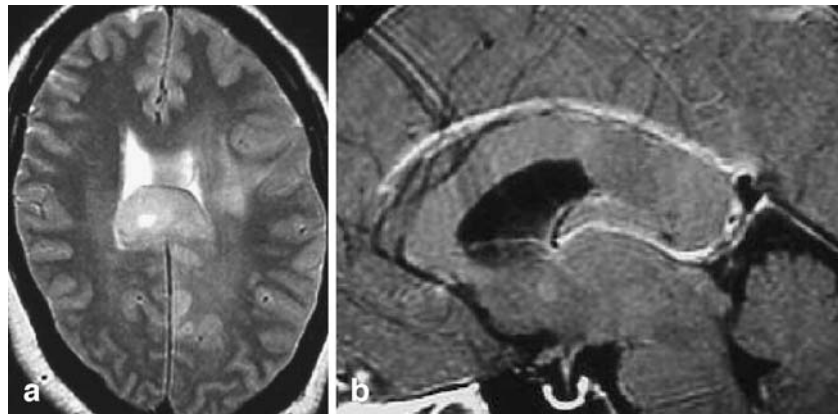


**Fig. 11** Gliomatosis cerebri in a 53-year-old woman. **a** T2-weighted axial image (TR/TE=4,000/104, 1.5 T) shows focal enlargement of the corpus callosum and diffuse abnormal signal intensity in the left hemisphere. **b** Post-contrast T1-weighted midsagittal image (TR/TE =616/12) shows no enhancement in the lesion, suggestive of benign glioma



most common histological type of astrocytoma, and it can occur at various sites in the central nervous system, including the corpus callosum. Moreover, fibrillary astrocytoma has a tendency to spread diffusely along white matter tracts such as the corpus callosum. The important MR finding in the differentiation of this lesion from glioblastoma is the lack of contrast enhancement (Fig. 11).

#### Lymphoma

The incidences of primary and secondary lymphoma of the central nervous system (CNS) are increasing. CNS lymphomas are almost always of the B-cell non-Hodgkin's type. Common locations include the corpus callosum, periventricular white matter and deep gray matter. Lymphomas are commonly multiple. Characteristic MR features of lymphoma in the CNS are homogeneous enhancement without central necrosis and relatively low signal intensity on T2-weighted images, reflective of

dense cellularity (Fig. 12). These MR features are useful in the differential diagnosis of lymphoma from glioma or metastatic tumor.

#### Metastasis

Metastasis directly to the corpus callosum is rare. Callosal involvement is usually a secondary spread from a metastatic focus in a neighboring structure such as the cingulate gyrus (Fig. 13).

#### Germinoma

Germ cell tumors usually arise from the pineal or suprasellar region. The corpus callosum is rarely involved [18]. When ependymal and subependymal dissemination develops, the inferior surface of the corpus callosum may be involved (Fig. 14).

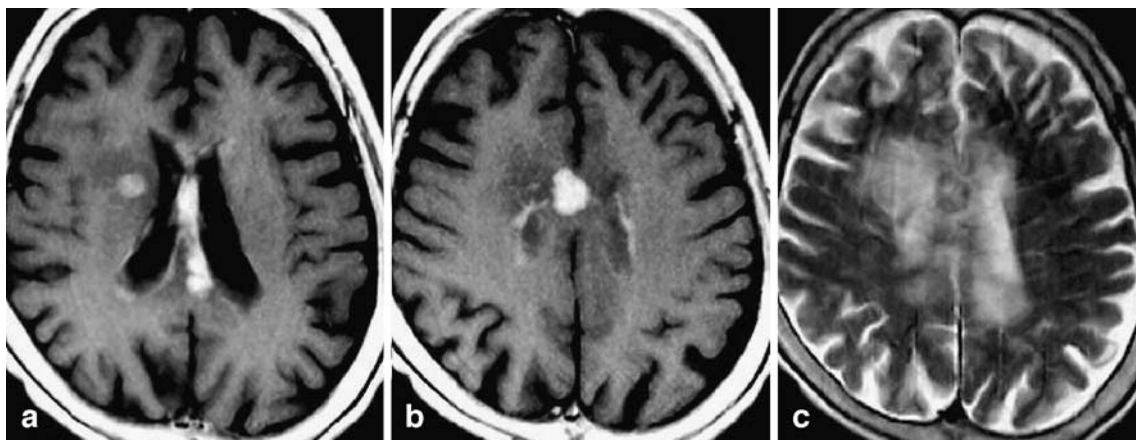


**Fig. 12** Lymphoma in a 72-year-old woman. **a, b** Post-contrast T1-weighted axial images (TR/TE=470/15, 1.0 T) show a strongly and homogeneously enhancing corpus callosal lesion with neighboring white matter lesions. **c** T2-weighted axial image (TR/TE=4,000/120)

shows the enhancing lesion to be isointense to slightly hyperintense relative to the gray matter. Widespread white matter abnormality is also seen



**Fig. 13** Metastatic brain tumor from a lung cancer in a 50-year-old man. Post-contrast T1-weighted midsagittal image (TR/TE=400/20, 1.5 T) shows an irregular enhancing mass in the left cingulate gyrus and corpus callosum. Pineal tumor is also detected

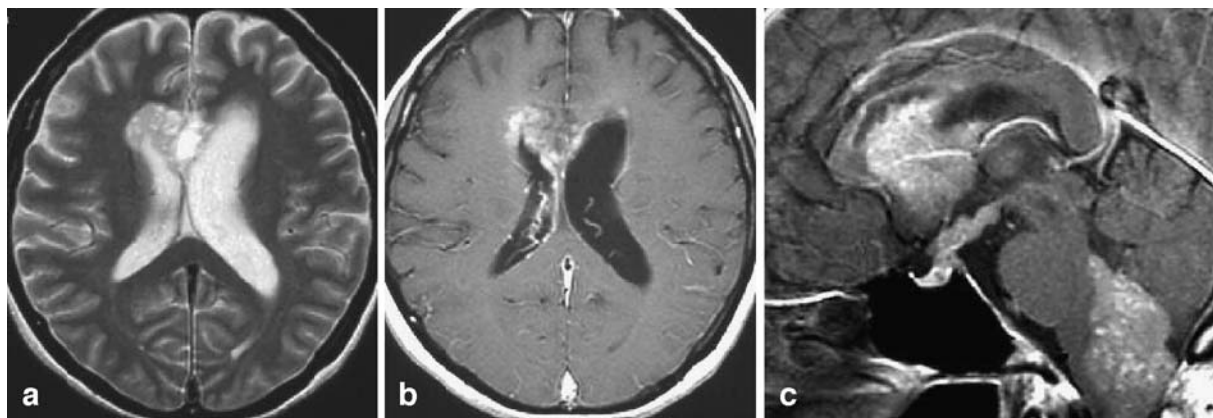


**Fig. 14** Germinoma with cerebrospinal fluid dissemination in a 45-year-old woman. **a** T2-weighted (TR/TE=4,000/80, 1.5 T) axial image shows an irregular mass lesion in the corpus callosum and around the right anterior horn of the lateral ventricle. **b, c** On post-

### Infections

Pathogens responsible for encephalitis show preferential sites of infection. For example, herpes simplex infects the temporal lobe. Viruses usually affect gray matter. The corpus callosum, which comprises white matter with dense fibers, is rarely affected. We encountered one patient with echovirus type-9 encephalitis affecting the corpus callosum (Fig. 15). Enteroviruses including echovirus type 9 are rare causes of acute focal encephalitis [19].

### Metabolic diseases

Metabolic diseases, for example, leukodystrophy, can involve the corpus callosum. Each type of leukodystrophy has a typical distribution of white matter lesions (Fig. 16).

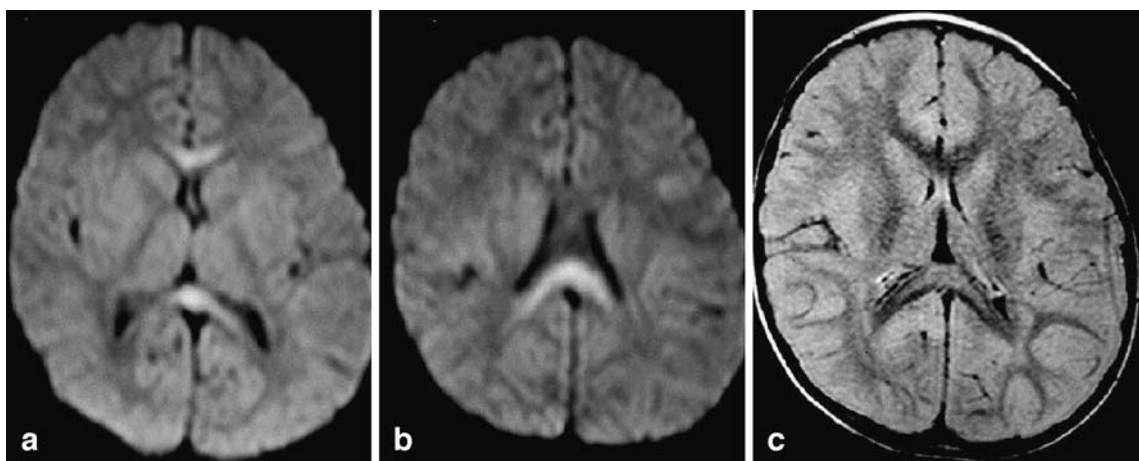


**Fig. 15** Echovirus type 9 encephalitis in a 3-year-old girl. **a, b** Diffusion-weighted (TR/TE=2,880/56, b=1,000, 1.5 T) axial images show hyperintense lesions in the genu and splenium of the

corpus callosum. **c** Axial FLAIR (TR/TI/TE=11,000/2,800/140) image shows a slightly hyperintense lesion in the splenium of the corpus callosum

**Fig. 16** Adult-onset globoid cell leukodystrophy in a 60-year-old woman. **a, b** Coronal FLAIR (TR/TI/TE=10,002/2,200/126.5, 1.5 T) images show white matter hyperintense lesions including the corpus callosum, corticospinal tracts and optic radiations. This is the typical distribution in Krabbe's disease

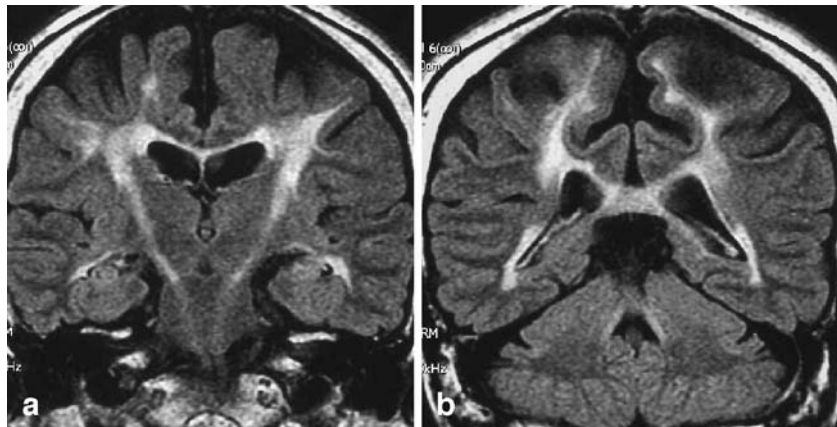
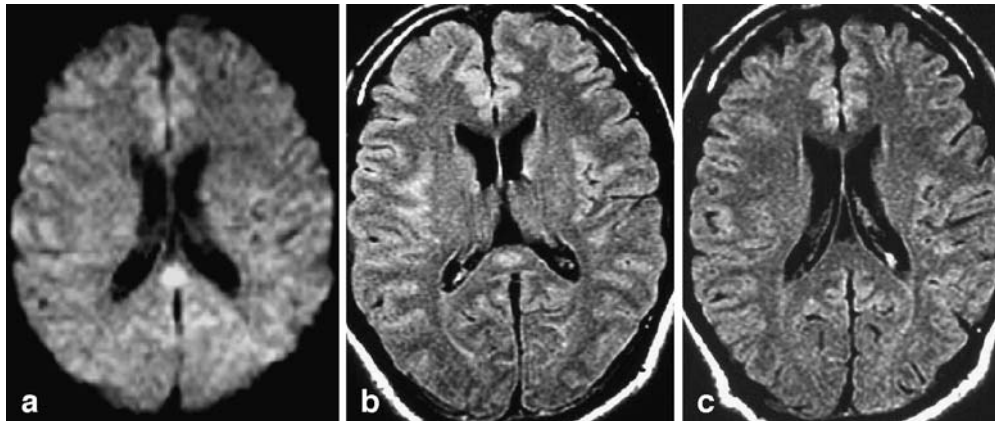


**Fig. 17** Transient splenial lesion in a 23-year-old man with tuberculous meningitis.

**a, b** Diffusion-weighted (TR/TE=4,000/101, b=1,000, 1.5 T) and FLAIR (TR/TI/TE=10,002/2,200/125) axial images show a focal ovoid lesion in the central splenium of the corpus callosum. **c** On a FLAIR image obtained 1 month after antituberculous chemotherapy, the lesion has disappeared



In the majority of cases of adrenoleukodystrophy, the splenium of the corpus callosum is involved [20].

patients with encephalitis (Fig. 17). Because these reversible focal lesions show markedly restricted diffusion, intracellular (intramyelinic) edema is regarded as the main pathologic abnormality [23].

## Miscellaneous lesions

### Transient splenial lesion

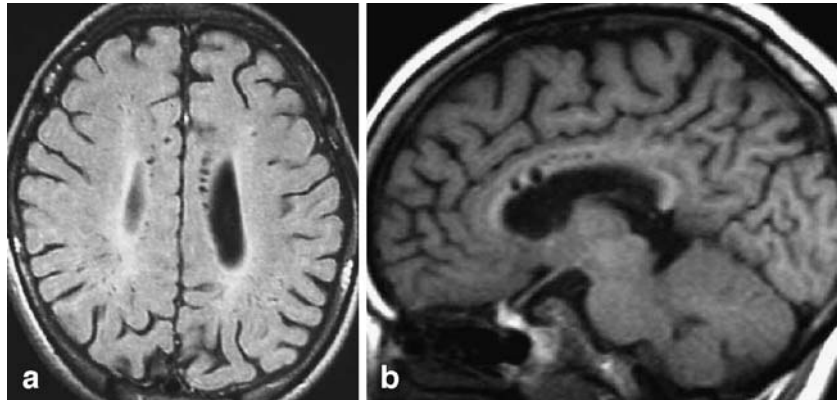
A transient ovoid or round lesion in the central splenium of the corpus callosum has recently been reported in epilepsy patients treated with antiepileptic drugs [21, 22] and in

### Dilated Virchow-Robin spaces

Unusually widened Virchow-Robin spaces are seen occasionally in the cerebral white matter, including the corpus callosum [24]. On FLAIR images, multiple small

**Fig. 18** Dilated Virchow-Robin spaces in a 6-year-old boy with psychomotor retardation.

**a** FLAIR axial image (TR/TI/TE=6,744/1,588/110, 1.0 T) shows multiple small, ovoid, cystic lesions in the left side of the corpus callosum. The cyst walls are not hyperintense. Periventricular hyperintensity with ventricular dilatation is also observed. **b** T1-weighted left parasagittal image (TR/TE=325/12) shows multiple cysts in the thin corpus callosum



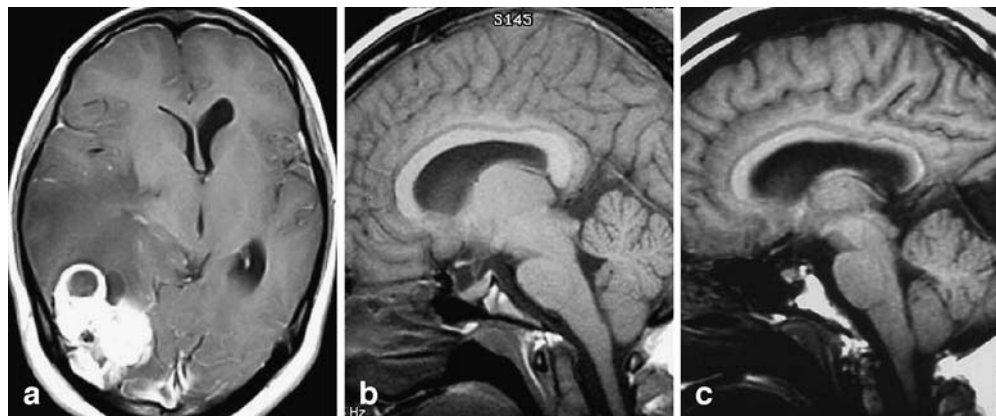


**Fig. 19** Wallerian degeneration of the corpus callosum in a 17-year-old girl with an anaplastic astrocytoma. **a** T1-weighted axial image (TR/TE=500/15, 1.0 T) with contrast shows a large tumor in the right temporo-occipital lobes. **b** T1-weighted midsagittal image (TR/TE=300/8, 1.5 T) obtained 6 days after surgery shows a normal

corpus callosum. **c** On a T1-weighted midsagittal image (TR/TE=300/14, 1.5 T) obtained 6 years after surgery, the posterior half of the corpus callosum is markedly atrophic, indicative of wallerian degeneration of the commissural fibers

ovoid cystic lesions containing cerebrospinal-like fluid without a wall of high-signal intensity are observed (Fig. 18). Usually, there is no neurological deficit relating to these lesions. Patients with mucopolysaccharidosis may also have dilated perivascular spaces.

#### Wallerian degeneration after hemispheric damage

After focal injury of the cerebral hemisphere, the related part of the corpus callosum becomes atrophic (Fig. 19). This atrophy is classified as wallerian degeneration of the commissural fibers [25].

#### Focal splenial gliosis

Focal linear hyperintense lesions in the anterior part of the splenium of the corpus callosum are frequently observed on FLAIR images in aged patients with subcortical arteriosclerotic encephalopathy and in patients who have undergone brain radiation therapy. This is a depiction of isomorphic gliosis [26]. According to Yamamoto et al. [27], this affected region is not subependymal, but subpial because the midanterior surface of the callosal splenium abuts the cistern of the velum interpositum, but not the ventricle. Sagittal and coronal FLAIR images are useful for the detection of callosal gliosis, which is correlated with periventricular hyperintensity and deep white matter

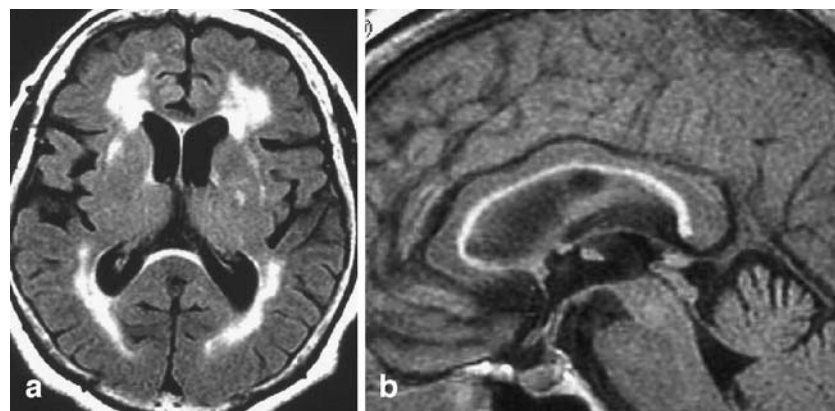


**Fig. 20** Focal splenial gliosis in a 72-year-old woman with subcortical arteriosclerotic encephalopathy. **a** FLAIR axial image (TR/TI/TE=10,002/2,200/133, 1.5 T) shows a hyperintense band in the anterior subependymal region of the splenium of the corpus callosum. Widespread periventricular hyperintensity, suggestive of

chronic ischemic white matter degeneration due to arteriosclerosis, is also observed. **b** On the midsagittal FLAIR image, there is a linear hyperintense lesion at the callosal-septal interface, including the anterior surface of the splenium

hyperintensity [28]. On midsagittal FLAIR images, the callosal-septal interface is linearly hyperintense in such patients (Fig. 20).

## Conclusion

Acquired corpus callosal lesions include vascular, traumatic, demyelinating, neoplastic and miscellaneous le-

sions. MR imaging is useful for the detection and differential diagnosis of corpus callosal lesions. Because these lesions are located close to the lateral ventricle, FLAIR images are most useful in their detection. Due to the anatomical shape and location of the corpus callosum, either coronal or sagittal images should be added in the evaluation of corpus callosal lesions.

## References

- Tench CR, Morgan PS, Wilson M, Blumhardt LD (2002) White matter mapping using diffusion tensor MRI. *Magn Reson Med* 47:967–972
- Friese SA, Bitzer M, Freudenstein D, Voigt K, Kuker W (2000) Classification of acquired lesions of the corpus callosum with MRI. *Neuroradiology* 42:795–802
- Bourekas EC, Varaklis K, Bruns D, Christoforidis GA, Baujan M, Slone HW, Kehagias D (2002) Lesions of the corpus callosum: MR imaging and differential considerations in adults and children. *AJR* 179:251–257
- Ture U, Yasargil G, Krisht AF (1996) The arteries of the corpus callosum: a microsurgical anatomic study. *Neurosurgery* 39:1075–1085
- Moody DM, Bell MA, Challa VR (1988) The corpus callosum, a unique white-matter tract: anatomic features that may explain sparing in Binswanger disease and resistance to flow of fluid masses. *Am J Neuroradiol* 9:1051–1059
- Kasow DL, Destian S, Braun C, Quintas JC, Kagetsu NJ, Johnson CE (2000) Corpus callosum infarcts with atypical clinical and radiologic presentations. *Am J Neuroradiol* 21:1876–1880
- Chrysikopoulos H, Andreou J, Roussakis A, Pappas J (1997) Infarction of the corpus callosum: computed tomography and magnetic resonance imaging. *Eur J Radiol* 25:2–8
- Auer DP, Putz B, Gossler C, Elbel GK, Gasser T, Dichgans M (2001) Differential lesion patterns in CADASIL and sporadic subcortical arteriosclerotic encephalopathy: MR imaging study with statistical parametric group comparison. *Radiology* 218:443–451
- Mendelsohn DB, Levin HS, Harward H, Bruce D (1992) Corpus callosum lesions after closed head injury in children: MRI, clinical features and outcome. *Neuroradiology* 34:384–388
- Ashikaga R, Araki Y, Ishida O (1997) MRI of head injury using FLAIR. *Neuroradiology* 39:239–242
- Hergan K, Schaefer PW, Sorensen AG, Gonzalez RG, Huisman TAGM (2002) Diffusion-weighted MRI in diffuse axonal injury of the brain. *Eur Radiol* 12:2536–2541
- Gean-Marton AD, Vezina LG, Marton KI, Stimac GK, Peyster RG, Taveras JM, Davis KR (1991) Abnormal corpus callosum: a sensitive and specific indicator of multiple sclerosis. *Radiology* 180:215–221
- Jackson A, Fitzgerald JB, Gillespie JE (1993) The callosal-septal interface lesions in multiple sclerosis: effect of sequence and imaging plane. *Neuroradiology* 35:573–577
- Palmer S, Bradley WG, Chen DY, Patel S (1999) Subcallosal striations: early findings of multiple sclerosis on sagittal, thin-section, fast FLAIR MR images. *Radiology* 210:149–153
- Feydy A, Carlier R, Mompoint D, Clair B, Chillet P, Vallee C (1997) Brain and spinal cord MR imaging in a case of acute disseminated encephalomyelitis. *Eur Radiol* 7:415–417
- Brass SD, Caramanos Z, Santos C, Dilenge ME, Lapierre Y, Rosenblatt B (2003) Multiple sclerosis vs acute disseminated encephalomyelitis in childhood. *Pediatr Neurol* 29:227–231
- Ruiz-Martinez J, Martinez Perez-Balsa A, Ruibal M, Urtasun M, Villanua J, Marti Masso JF (1999) Marchiafava-Bignami disease with widespread extracallosal lesions and favourable course. *Neuroradiology* 41:40–43
- Liang L, Korogi Y, Sugahara T, Ikushima I, Shigematsu Y, Okuda T, Takahashi M, Kochi M, Ushio Y (2002) MRI of intracranial germ-cell tumours. *Neuroradiology* 44:382–388
- Zuckerman MA, Sheaff M, Martin JE, Gabriel CM (1993) Fatal case of echovirus type 9 encephalitis. *J Clin Pathol* 46:865–866
- Loes DJ, Hite S, Moser H, Stillman AE, Shapiro E, Lockman L, Latchaw RE, Kravit W (1994) Adrenoleukodystrophy: a scoring method for brain MR observations. *Am J Neuroradiol* 15:1761–1766
- Feitova V, Feit J, Krupa P (2002) Therapy-related change of corpus callosum in a young patient with epilepsy. *Eur Radiol* 12:345–347
- Maeda M, Shiroyama T, Tsukahara H, Shimono T, Aoki S, Takeda K (2003) Transient splenial lesion of the corpus callosum associated with antiepileptic drugs: evaluation by diffusion-weighted MR imaging. *Eur Radiol* 13:1902–1906
- Takanashi J, Barkovich AJ, Yamaguchi K, Kohno Y (2004) Influenza-associated encephalitis/encephalopathy with a reversible lesion in the splenium of the corpus callosum: a case report and literature review. *Am J Neuroradiol* 25:798–802
- Ogawa T, Okudera T, Fukasawa H, Hashimoto M, Inugami A, Fujita H, Hatazawa J, Shimosegawa E, Noguchi K, Uemura K, Nakajima S, Yasui N (1995) Unusual widening of Virchow-Robin spaces: MR appearance. *Am J Neuroradiol* 16:1238–1242
- Uchino A, Kato A, Yuzuriha T, Takashima Y, Kudo S (2001) Cranial MR imaging of sequelae of prefrontal lobotomy. *Am J Neuroradiol* 22:301–304
- Pekala JS, Mamourian AC, Wishart HA, Hickey WF, Raque JD (2003) Focal lesion in the splenium of the corpus callosum on FLAIR MR images: a common finding with aging and after brain radiation therapy. *Am J Neuroradiol* 24:855–861
- Yamamoto A, Miki Y, Fushimi Y, Okada T, Tomimoto H (2004) Mid-anterior surface of the callosal splenium: subependymal or subpial? *Am J Neuroradiol* 25:664–665
- Yamamoto A, Miki Y, Tomimoto H, Kanagaki M, Takahashi T, Fushimi Y, Konishi J, Haque TL, Togashi K (2005) Age-related signal intensity changes in the corpus callosum: assessment with three orthogonal FLAIR images. *Eur Radiol* 15:2304–2311